

수소/산소 연료시스템에서의 충격관-자외선
흡수분광법을 이용한 $\text{H} + \text{O}_2 = \text{OH} + \text{O}$ 기체상 반응연구

류시욱, 황순목
Department of Chemical Engineering,
The University of Toledo,
Toledo, OH 43606,

M. J. Rabinowitz*
Internal Fluid Mechanics Division*
NASA Lewis Research Center
Cleveland, OH 44135

**Gas Phase Reaction Study of $\text{H} + \text{O}_2 = \text{OH} + \text{O}$ in H_2/O_2 Fuel System by
Shock Tube-Laser Absorption Spectroscopic Technique**

S. -O. Ryu, S. M. Hwang
Department of Chemical Engineering,
The University of Toledo,
Toledo, OH 43606,

M. J. Rabinowitz*
Internal Fluid Mechanics Division*
NASA Lewis Research Center
Cleveland, OH 44135

Introduction

The title reaction is the main chain branching reaction in the oxidation of hydrogen and hydrocarbon based fuels. About 80% of the oxygen in a typical atmospheric pressure hydrocarbon flame is consumed by this reaction.¹ Thus, ignition delays and flame speeds are invariably found to be sensitive to the rate coefficient of this reaction.

The central role of the reaction in combustion has made it the object of intense scrutiny. In 1972 Baulch et al.² (BDHL) reviewed the available data and recommended the rate coefficient expression $k_1 = 2.2 \times 10^{14} \exp(-8450 \text{ K/T}) \text{ cm}^3 \text{ mol}^{-1} \text{ s}^{-1}$. In 1973 Schott³ measured the exponential growth rate of CO_2 chemiluminescence in shock heated $\text{H}_2/\text{CO}/\text{O}_2/\text{Ar}$ mixtures and reported a rate coefficient expression with a temperature dependent pre-exponential factor, $k_1 = 1.22 \times 10^{17} \text{ T}^{-0.907} \exp(-8369 \text{ K/T}) \text{ cm}^3 \text{ mol}^{-1} \text{ s}^{-1}$. For over a decade these two expressions formed the upper, BDHL, and lower, Schott, accepted limits for k_1 , differing by a factor of 1.7 at 2000 K. In 1984 Warnatz¹ reviewed the available data and recommended Schott's expression. In 1985 Frank and Just⁴ measured O- and H-atom concentration profiles in shock heated $\text{H}_2/\text{O}_2/\text{N}_2\text{O}/\text{Ar}$ mixtures and reported a rate coefficient expression $k_1 = 2.44 \times 10^{14} \exp(-8697 \text{ K/T}) \text{ cm}^3 \text{ mol}^{-1} \text{ s}^{-1}$, which agreed well with the recommended value of BDHL; no temperature dependence of the pre-exponential factor was found. This prompted a flurry of experimental and theoretical investigations of the title reaction using more advanced diagnostics and techniques.

Even though numerous experimental studies have been performed, disagreement still exists among the reported values of k_1 . In this study we performed a series of experiments over a wide range of composition and pressure to address these issues.

Experimental

The experimental setup has been described in detail previously.⁵ Experiments were performed in a rolled square stainless steel shock tube 6.35 cm in cross-section. Shocks were initiated by mechanically bursting an aluminum diaphragm with a cross shaped knife edge plunger. A combined leak and outgassing rate of $5 \times 10^{-6} \text{ Torr min}^{-1}$ was measured. Shock properties were computed using measured incident shock velocities extrapolated to the end wall and standard methods⁶ assuming full vibrational relaxation and no chemical reaction at the shock front. NASA thermochemical data were used throughout the calculations. Temperature and density were corrected for the effect of shock/boundary layer interaction following the methodology of Michael and Sutherland,⁷ resulting in an average 1.4% increase in temperature. The temporal profile of OH concentration was monitored using the $\text{P}_1(5)$ line of the (0,0) band of the $\text{A}^2\Sigma^+ \leftarrow \text{X}^2\Pi$ transition at 310.032 nm (air). Intracavity doubling crystal of a dye laser produced a single mode 5 mW UV beam with a 2 mm beam

diameter. Center wavelength of the OH absorption line was determined by passing part of the UV beam through a burner stabilized CH₄/Air flame. A double-beam scheme was employed for signal detection. The test gas mixtures were prepared manometrically and allowed to stand for 48 h before use. Test gases were used without further purification, stated purities were: H₂, 99.9995% (Linde Research Grade, THC as CH₄<0.3 ppm), O₂, 99.6% (Linde Zero Grade, THC as CH₄<0.3 ppm), Ar, 99.996% (Linde Zero Grade, THC as CH₄<0.3 ppm).

Results and discussion

Typical transmission profiles at different experimental conditions are shown in Figure 1. After an induction period light absorption increases rapidly due to the essentially exponential growth of OH concentration caused by chain branching and propagation reactions. Data reduction was accomplished using a small set of relevant information derived from the absorption traces, namely: $A_{max} = (1 - I/I_0)_{max}$, normalized maximum slope, $NS_{max} = -d((I/I_0)/dt)_{max}/A_{max}$, and one characteristic time, t_{50} , the time to reach 50% of A_{max} . These three observables were chosen based upon sensitivity analysis using a trial H₂/O₂ reaction mechanism. Eight rich mixtures of equivalence ratios of 2, 5, and 10 were used in the experiments. Reflected shock temperatures and pressures ranged from 1050 to 2500 K and from 0.7 to 4.0 atm, respectively.

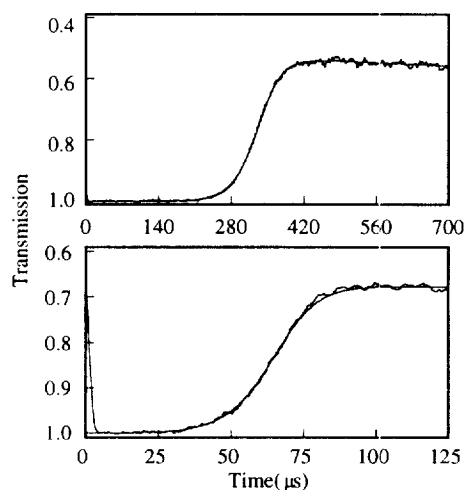


Figure 1. Typical experimental records. (top) 2.0% H₂, 0.5% O₂, 97.5% Ar, T₅ = 1556 K, and P₅ = 0.75 atm. (bottom) 2.0% H₂, 0.2% O₂, 97.8% Ar, T₅ = 2163 K, and P₅ = 1.99 atm. Spikes at time zero are schlieren signals due to reflected shock front passage. Smooth lines are computed OH absorption profiles using the mechanism and the OH absorption coefficients determined from A_{max} .

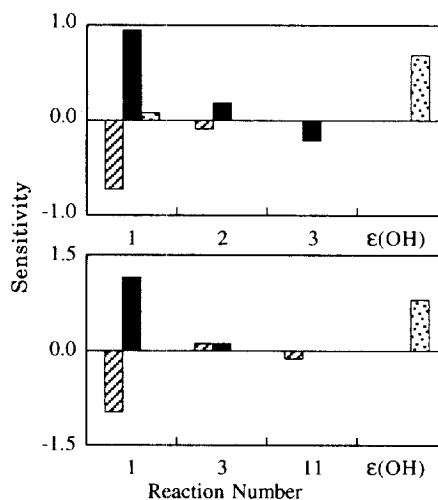


Figure 2. Sensitivity spectra for the experimental conditions in Figure 1. Sensitivities are for 30% increase to rate coefficient values in the present reaction mechanism and absorption coefficients. Reaction numbers are listed in reference 5. Filled for NS_{max} sensitivity, dotted for A_{max} sensitivity, and hashed column for t_{50} sensitivity.

Computer simulations were performed using the detailed reaction mechanism of Yuan et al.⁸(YWYFR) with modifications. The reaction mechanism and rate coefficient expressions are given in detail previously.⁵ Reverse reaction rate coefficients were calculated from the principle of detailed balancing. NASA thermochemical data were used in all calculations. The LSODE integration package was used to solve the set of stiff differential equations describing chemical reaction under the assumed constant density conditions for reflected shocks. Local logarithmic response sensitivities⁹ computed for the Figure 1 experimental conditions are shown in Figure 2. Overall, NS_{max} and t_{50} are sensitive only to the title reaction. Therefore, k_1 could be determined by matching NS_{max} or t_{50} .

Based upon the sensitivity and contaminant effect studies k_1 and $\epsilon(\text{OH})$ were the parameters chosen for simultaneous optimization using NS_{max} and A_{max} as the target criteria. The data obtained above 2500 K were not included in the analysis due to possible contamination effects. However, as can be seen in Figure 3, these points lie on the extrapolated line. A least squares fit to the data is given by $k_1(\text{NS}_{\text{max}}) = (7.13 \pm 0.31) \times 10^{13} \exp(-6957 \pm 30 \text{ K/T}) \text{ cm}^3 \text{ mol}^{-1} \text{ s}^{-1}$, with a 4% standard deviation, over the temperature range 1050 to 2500 K. k_1 and $\epsilon(\text{OH})$ also can be determined using t_{50} and A_{max} as the optimization criteria. Results of this analysis are shown in Figure 4 where the solid line represents the least squares fit to the data given by $k_1(t_{50}) = (7.19 \pm 0.41) \times 10^{13} \exp(-7015 \pm 40 \text{ K/T}) \text{ cm}^3 \text{ mol}^{-1} \text{ s}^{-1}$, with a 6% standard deviation, over the same temperature range. The choice of optimization criteria results in two slightly different Arrhenius expressions that diverge with decreasing temperature for a maximum difference of 5% at the low temperature extreme. The agreement of these two expressions implies that our experimental results were not significantly influenced by the presence of impurities. Maximum uncertainties in the determination of $k_1(\text{NS}_{\text{max}})$ and $k_1(t_{50})$ were 6.0% and 7.5% respectively.

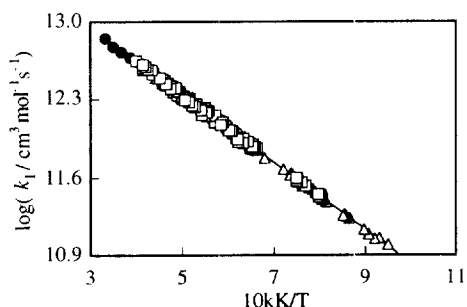


Figure 3. Arrhenius plot of the experimental data for $k_1(\text{NS}_{\text{max}})$. The solid line is the least squares fit to the data. Symbols are triangles for $\phi = 2$ mixtures, squares for $\phi = 5$ mixtures, circles for $\phi = 10$ mixture, and filled circles for $\phi = 15$ mixture. The data for $\phi = 15$ mixture were not included in the least squares fit for $k_1(\text{NS}_{\text{max}})$.

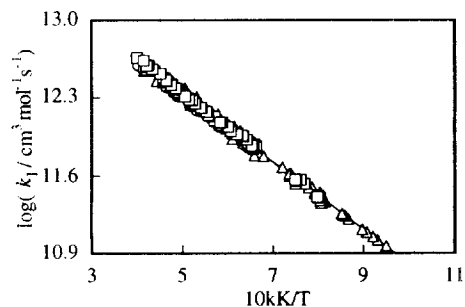


Figure 4. Arrhenius plot of the experimental data for $k_1(t_{50})$. The solid line is the least squares fit to the data. Symbols as in Figure 3.

A profile computed using the present reaction mechanism is shown in Figure 1 as the smooth line. The mechanism reproduces the experimental profile quite well. Similar fidelity of match is obtained for the other experimental conditions. The present determination of k_1 is compared to recent experimental and modeling studies in Table 1.

Table 1. Comparison of rate coefficient expressions^a

| authors ^b | T range | A | n | θ | ref | notes |
|----------------------|-----------|-----------------------|--------|----------|------------|-------|
| PMSK | 962-1750 | 1.68×10^{14} | 0.00 | 8119 | 10 | |
| MHB | 1450-3370 | 9.33×10^{13} | 0.00 | 7448 | 11 | |
| YWYFR | 1050-2700 | 1.59×10^{17} | -0.927 | 8493 | 8 | |
| SM | 1103-2055 | 6.93×10^{13} | 0.00 | 6917 | 12 | |
| DH | 960-5300 | 9.76×10^{13} | 0.00 | 7474 | 13 | c |
| YFMHB | 1336-3370 | 8.30×10^{13} | 0.00 | 7253 | 14 | d |
| YGSF | 1100-3550 | 7.60×10^{13} | 0.00 | 7065 | 15 | e |
| RHR | 1050-2500 | 7.13×10^{13} | 0.00 | 6957 | This Study | |

^aRate coefficients are in the form $k = A T^n \exp(-\theta / T)$. Units are K, cm^3 , mol, and s. ^bAbbreviations explained in text. ^ccombined results with SM, MHB, PMSK data. ^doptimization using YWYFR and MHB data, ^ecombined results with SM data.

Non-zero experimental values are reported by Schott (-0.907), YWYFR (-0.927), and Masten et al. (MHB) (-0.7, obtained from the combination of MHB and Pirraglia et al.¹⁰ (PMSK) data). PMSK, MHB (MHB data only), Shin and Michael (SM), Du and Hessler

(DH), Yu et al. (YFMHB), Yang et al. (YGSF) and the present study (RHR) do not find a temperature dependence for the pre-exponential factor. Recently Varandas et al.¹⁶ (VBP) calculated the thermal rate coefficient theoretically. Their calculations showed no temperature dependence for the pre-exponential factor. The expressions of the present study and that of SM¹² are in good agreement over the temperature range 1100-2055 K. We do not support curvature in k_1 .

There exists reasonable agreement between the results of this study and most of the recent evaluations of $k_1^{10,12-15}$ and so it is possible to achieve a consensus expression given by $k_1=7.82 \times 10^{13} \exp(-7105 \text{ K/T}) \text{ cm}^3 \text{ mol}^{-1} \text{ s}^{-1}$ over the temperature range 960 to 5300 K, with an uncertainty of 6%.

Conclusions

The rate coefficient of the reaction $\text{H}+\text{O}_2=\text{OH}+\text{O}$ was determined using OH laser absorption spectroscopy behind reflected shock waves over the temperature range 1050-2500 K and the pressure range 0.7 - 4.0 atm. Two distinct and independent criteria were employed in the evaluation of k_1 , namely NS_{max} and t_{50} . Our recommended expression for k_1 , obtained using NS_{max} , is $k_1=7.13 \times 10^{13} \exp(-6957 \text{ K/T}) \text{ cm}^3 \text{ mol}^{-1} \text{ s}^{-1}$. This expression agrees with that of SM and with the computational results of VBP. We neither support a curved rate coefficient expression nor do we find evidence of composition dependence upon the determination of k_1 . Critical review of recent k_1 determinations yields the consensus expression $k_1=7.82 \times 10^{13} \exp(-7105 \text{ K/T}) \text{ cm}^3 \text{ mol}^{-1} \text{ s}^{-1}$ over the temperature range 960 to 5300 K.

Acknowledgement

S-OR and SMH gratefully acknowledge the support of NASA Grant NAG3-1307.

References

1. Warnatz, J.: "Combustion Chemistry", Gardiner, W. C., Jr., Ed., Chapter 5, Springer-Verlag, New York, NY(1984).
2. Baulch, D. L., Drysdale, D. D., Horne, D. G. and Lloyd, A. C.: "Evaluated Kinetic Data for High Temperature Reactions", Vol. 1, Butterworths, London, England(1972).
3. Schott, G. L.: *Combust. Flame*, 21, 357(1973).
4. Frank, P. and Just, Th.: *Ber. Bunsenges. Phys. Chem.*, 89, 181(1985).
5. Ryu, S. -O.: Ph. D. Dissertation, University of Toledo, Toledo, OH(1994).
6. Gardiner, W. C., Jr., Walker, B. F. and Wakefield, C. B.: "Shock Waves in Chemistry", Lifshitz, A., Ed., Chapter 7, Marcel Dekker: New York, NY(1981).
7. Michael, J. V. and Sutherland, J. W.: *Int. J. Chem. Kinet.*, 18, 409(1986).
8. Yuan, T., Wang, C., Yu, C. L., Frenklach, M. and Rabinowitz, M. J.: *J. Phys. Chem.* 95, 1258(1991).
9. Gardiner, W. C., Jr.: *J. Phys. Chem.* 81, 2367(1977).
10. Pirraglia, A. N., Michael, J. V., Sutherland, J. W. and Klemm, R. B.: *J. Phys. Chem.* 93, 282(1989).
11. Masten, D. A., Hanson, R. K. and Bowman, C. T.: *J. Phys. Chem.* 94, 7119(1990).
12. Shin, K. S. and Michael, J. V.: *J. Chem. Phys.* 95, 262(1991).
13. Du, H. and Hessler, J. P.: *J. Chem. Phys.* 96, 1077(1992).
14. Yu, C. -L., Frenklach, M., Masten, D. A., Hanson, R. K. and Bowman, C. T.: *J. Phys. Chem.* 98, 4770(1994).
15. Yang, H., Gardiner, W. C., Jr., Shin, K. S. and Fujii, N.: *Chem. Phys. Lett.* 231, 449(1994).
16. Varandas, A. J. C., Brandao, J. and Pastrana, M. R.: *J. Chem. Phys.* 96, 5137(1992).